Broadband finite-difference Q-compensation engine for accurate Q-RTM

Tong Zhou, Michigan State University; Wenyi Hu, Advanced Geophysical Technology Inc.; Jieyuan Ning, Peking University

Summary

We developed an efficient finite-difference Q-RTM algorithm applicable to acoustic tilted transversely isotropic (TTI) scenarios in a broadband sense (~5 - 70 Hz). Compared to our previously reported method with a multi-stage optimization technique for dispersion relation preservation during back-propagation, the new method further extends the applicable frequency range down to 5 Hz, thus the new algorithm is able to compensate the Q effects accurately for the low frequency signals that are often critical for subsurface imaging. This broadband Q-RTM algorithm is based on the finite-difference method, which simplifies the procedure of parallel computing with GPUs, especially for large scale projects. The broadband dispersion relation preservation during the Q-compensation process is realized by introducing extra time-domain integration optimization terms to either the real or the imaginary part of the complex modulus. This method is validated by the theoretical analysis and the numerical experiments. The results are comparable to a regular finite-difference RTM without Q (serving as the reference solution), with all the missing structural information recovered and the blurred events refocused accurately.

Introduction

Strong attenuation on fluid-saturated reservoirs and gas clouds impose challenges on seismic imaging with conventional migration methods, observed as dimming or missing structures below the visco-acoustic overburdens, reduced spatial resolution, wrong structure depth and polarity due to the traveltime error and wavelet shape distortion. Q-compensation technologies have been developed to improve the imaging quality, including the inverse Q filtering (Bickel and Natarajan, 1985; Hargreaves, 1991), the Kirchhoff Q-migration (Traynin et al., 2008), Q-WEM (One-way wave equation Q-migration, Dai and West, 1994; Yu et al., 2002), and Q-RTM. Powered by full waveform forward modeling as the propagation engine, Q-RTM (Zhang et al., 2010; Zhu et al., 2014; Hu et al., 2016) is believed to be the most accurate imaging method for complicated geological settings with attenuation.

Most of the existing Q-RTM algorithms are based on the decoupling of the amplitude and the phase by the fractional differential method (Zhang et al., 2010; Zhu et al., 2014). This category of methods employs global pseudo-spectral operators (i.e., FFT and inverse FFT) to evaluate the fractional derivatives in the governing equations of Q-compensated wave propagation. For large industrial-sized 3D projects, domain decomposition is often a necessary strategy for the purpose of parallelization, which substantially increases the complexity level of the code modification for the global-operator-based methods. Besides, the limited size of the shared memory on GPUs prohibits the usage of global stencils, thus the high-efficiency implementation on GPU is extremely hard for global operators. Due to this fact, a Q-RTM approach based on local operators (e.g., finite difference method) is more preferable. Unfortunately, a direct adaptation of the finite-difference Q-attenuation propagator (Blanch et al., 1995) for Q-compensation use is either unstable or even further distort the phase shift caused by the attenuation (Guo et al., 2016).

Our previously developed Q-RTM method (Hu et al., 2016, 2017; Zhou et al., 2018a, b) successfully solved that problem by first applying a negative τ method to stably boost the amplitude and then introducing the multi-stage optimization terms to the real part of the complex modulus for correcting the phase with high accuracy in the preset frequency range. Only integer order derivative terms are used for the dispersion relation optimization (i.e., phase velocity correction) to maintain the local property of the numerical differential operators. Due to the limitation of polynomial regression, the valid frequency range for this method is approximately 15 - 70 Hz in which the phase velocity error is controlled within 1%. In this work, we extend the method by introducing a unique time domain integral term into the governing equations, which adds more degrees of freedom to the dispersion relation optimization. The new method is able to accurately compensate both the amplitude and the phase in a wider frequency range (~ 5 - 70 Hz). Besides, the numerical evaluation of the extra integral term is straightforward and efficient with the aid of an additional auxiliary PDE, without ruining the local-operator-based nature of the method. The overhead in the computational cost brought by the extra integral term is negligible.

Broadband finite-difference Q-compensated wave equation

In Q-RTM, the attenuation effect needs to be replaced by the Q-compensation for both the source-side and receiver-side propagation. Consequently, the key component of Q-RTM method is an accurate Q-compensated wave propagation engine to revert the Q attenuation effects. We apply the generalized standard linear solid (GSLS) visco-acoustic model to build this Q-compensated wave equation in order to maintain the localized nature of the numerical differential operators. The governing equations for Q-attenuation using the GSLS method are (Blanch et al., 1995):

$$\frac{\partial v}{\partial t} = -\frac{1}{\rho}\nabla p$$
$$-\rho\frac{\partial p}{\partial t} = M_0(1 + L\tau)\nabla \cdot v + \sum_{l=1}^{L} r_l \qquad (1)$$
$$\frac{\partial r_l}{\partial t} = -\tau\frac{M_0}{\tau_{\sigma l}}\nabla \cdot v - \frac{1}{\tau_{\sigma l}} r_l$$

where p is the pressure, v is the particle velocity; M_0 is the relaxed modulus (long-term elasticity feature); ρ is the density; L is the number of relaxation mechanisms. τ is a dimensionless parameter dependent on Q. $\tau_{\sigma l}$ are the stress relaxation times of each relaxation mechanism, respectively. The distribution of $\tau_{\sigma l}$ is determined by the frequency range. r_l are memory variables introduced to simulate the accumulated attenuation effects without employing the convolution operator (Carcione et al., 1988; Robertsson et al., 1994). By converting equation (1) to the frequency domain we obtain the complex modulus:

$$M(\omega) = M_0\left[1 + L\tau - \sum_{l=1}^{L}\frac{\tau}{1+\omega^2\tau_{\sigma l}^2} + \sum_{l}^{L}\frac{i\omega\tau\tau_{\sigma l}}{1+\omega^2\tau_{\sigma l}^2}\right] \qquad (2)$$

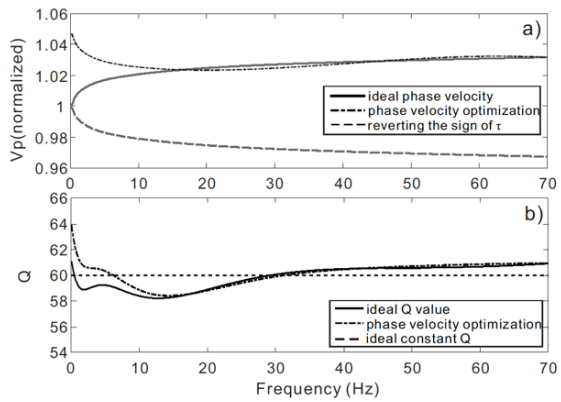

Figure 1. Phase velocity a) and absolute Q value b) of reverting the sign of τ, and previous multi-stage optimization method (non-broadband phase velocity compensation).

The real part of the complex modulus represents the phase effect while the imaginary part of the complex modulus represents the amplitude effect. The corresponding Q and phase velocity can be expressed as:

$$Q(\omega) = \frac{\Re\big(M(\omega)\big)}{\Im\big(M(\omega)\big)} = \frac{1 + L\tau - \sum_{l=1}^{L}\frac{\tau}{1+\omega^2\tau_{\sigma l}^2}}{\sum_{l=1}^{L}\frac{\omega\tau\tau_{\sigma l}}{1+\omega^2\tau_{\sigma l}^2}} \qquad (3)$$
$$c_p(\omega) \approx \sqrt{\Re\big(M(\omega)\big)} = c_0\left[1 + L\tau - \sum_{l=1}^{L}\frac{\tau}{1+\omega^2\tau_{\sigma l}^2}\right]$$

where $c_0 = \sqrt{M_0/\rho}$ is the zero-frequency reference velocity.

In our previous work, the sign of τ is flipped to obtain a negative Q (boosting the amplitude) while the frequency domain polynomial optimization terms $\alpha_0 + \alpha_2\omega^2 + \alpha_4\omega^4$ are added to the real part of the complex modulus, intending to correct the phase velocity distortion caused by reverting the sign of τ. However, the performance of this optimization term deteriorates rapidly as the frequency drops under 15 Hz (Figure 1, dash-dotted line).

The deviation of the phase velocity in the low frequency ranges (below 15 Hz) is due to the lack of degree of freedom of the polynomial optimization terms. In order to further extend the effective frequency range, we introduce a new set of optimization terms $\alpha_0 + \alpha_2\omega^2 + \alpha_4\omega^4 + \alpha_{-2}\omega^{-2}$.

The newly added term $\alpha_{-2}\omega^{-2}$ increases the degrees of freedom of the optimization, resulting in significantly improvement of the dispersion curve fitting in the low frequency range. The optimization parameters $\alpha_0, \alpha_2, \alpha_4, \alpha_{-2}$ are obtained by solving the optimization problem minimizing the least-square misfit of the optimized phase velocity and the ideal phase velocity (i.e., the phase velocity in lossy media) in a certain frequency range, which is equivalent to:

$$\min\left|\Re\left[M'^{(\omega,\alpha_0,\alpha_2,\alpha_4,\alpha_{-2})}\right] - \Re[M(\omega)]\right|_2^2, \quad \text{s.t. } \omega \in [\omega_a, \omega_b] \qquad (4)$$

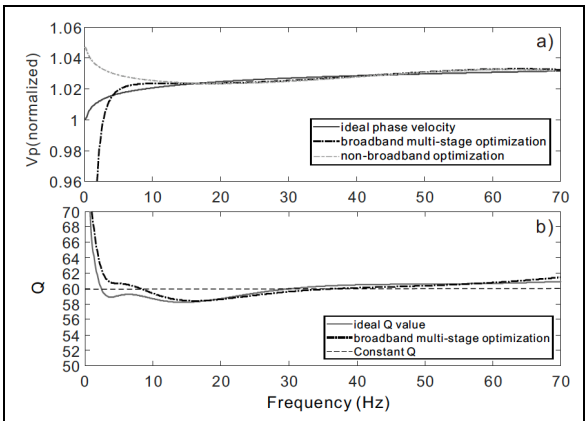

Figure 2. Phase velocity a) and absolute Q value b) of the broadband Q-compensated wave equation. As a reference, the non-broadband phase velocity optimization result is plotted in light gray dash-dotted line in subfigure a).

The dispersion relation optimization results for the scenario of Q=60 is shown in Figure 2. Compared to our previously reported method, this method successfully extends the effective frequency range of Q-compensation to as low as 3-5 Hz, which could be a very important feature for seismic imaging.

Finally, the time-domain wave equations ready for implementation are:

$$\frac{\partial^2 p}{\partial t^2} = (1 - L\tau)c^2\nabla^2(p + p^C) - \sum_{l=1}^{L} s_l + r$$
$$\frac{\partial s_l}{\partial t} = -\frac{\tau}{\tau_{\sigma l}} c^2\nabla^2 p - \frac{1}{\tau_{\sigma l}} s_l \qquad (6)$$
$$\frac{\partial^2 r}{\partial t^2} = c^2\alpha_{-2}\nabla^2 p$$
$$p^C = \alpha_0 p - \alpha_2 c^2\nabla^2 p + \alpha_4 c^2\nabla^2(c^2\nabla^2 p)$$

Optimizing the Q value

An alternative approach for broadband Q-compensation algorithm design is to keep the phase velocity fixed (the real part of the complex modulus) and introduce optimization terms to the imaginary part of the complex modulus to obtain an accurate negative Q value, thus boosting the amplitude without modifying the phase velocity during the back-propagation process (Zhou et al., 2018b). To fulfill such a requirement, again we add an integral optimization term to the imaginary part of the complex modulus: $\alpha_{-1}\omega^{-1} + \alpha_1\omega + \alpha_3\omega^3 + \alpha_5\omega^5 + \alpha_7\omega^7$. Figure 3 shows the dispersion relation optimization result using this scheme. The main advantage of this approach is that the phase velocity for Q-compensation is error-free in the whole frequency range, alleviating concerns over the migration position error. However, the Q value optimization error is larger (10%~15% of the Q value), which may cause some wavelet distortion after the Q-compensation though this type of distortion is insignificant according to our observation.

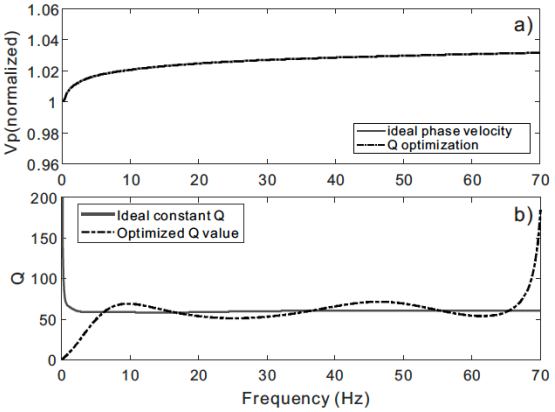

Figure 3. Phase velocity a) and Q value b) of the broadband Q-compensated wave equation by optimizing the Q value. The phase velocity curve is nearly identical to the ideal phase velocity, so the two curves coincide in subfigure a).

Low-frequency waveform recovery test

Figure 4 shows the waveform recovery testing result of the broadband Q-compensation scheme with Ricker source wavelets with dominant frequency of 10 Hz. The wavelet is propagated in a Q=60 media from the source location to the receiver for 1400 meters. After that, the time reversed recorded signals are back-propagated in the same media using the three Q-compensation approaches: 1) the previously reported multi-stage optimization scheme for Q-compensation; 2) the broadband Q-compensation scheme with the real part modulus optimization; 3) the broadband Q-compensation scheme with the imaginary part modulus optimization.

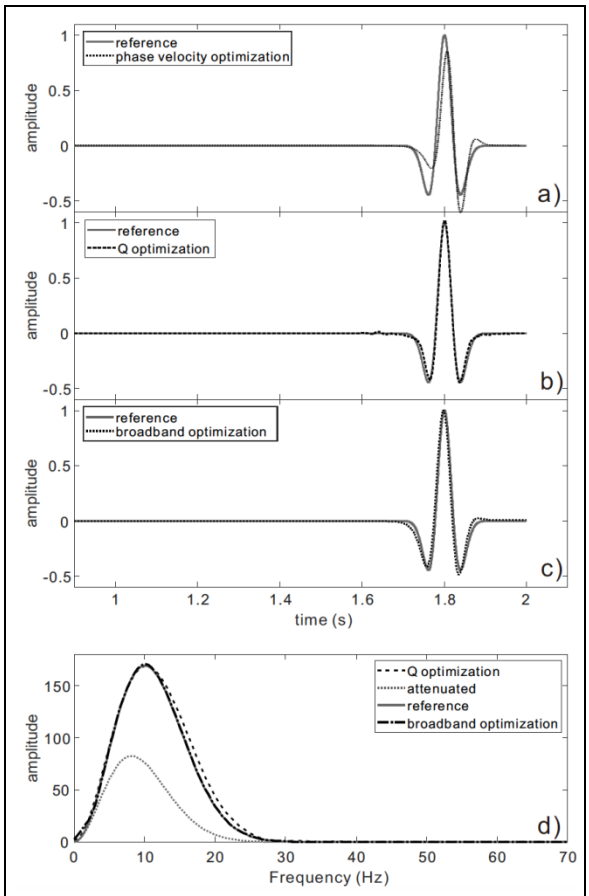

Figure 4. Waveform recovery test with 10 Hz wavelet. a) previous Q-RTM with multi-stage optimization; b) broadband Q-RTM optimizing the Q value; c) broadband Q-RTM optimizing the phase velocity; d) Amplitude spectrum of a), b) and c).

The previously reported method results in severe wavelet asymmetry because of the relatively large phase velocity error in the low frequency band 5 - 10 Hz (Figure 1). Instead,

both the broadband methods exhibit nearly complete wavelet shape recovery.

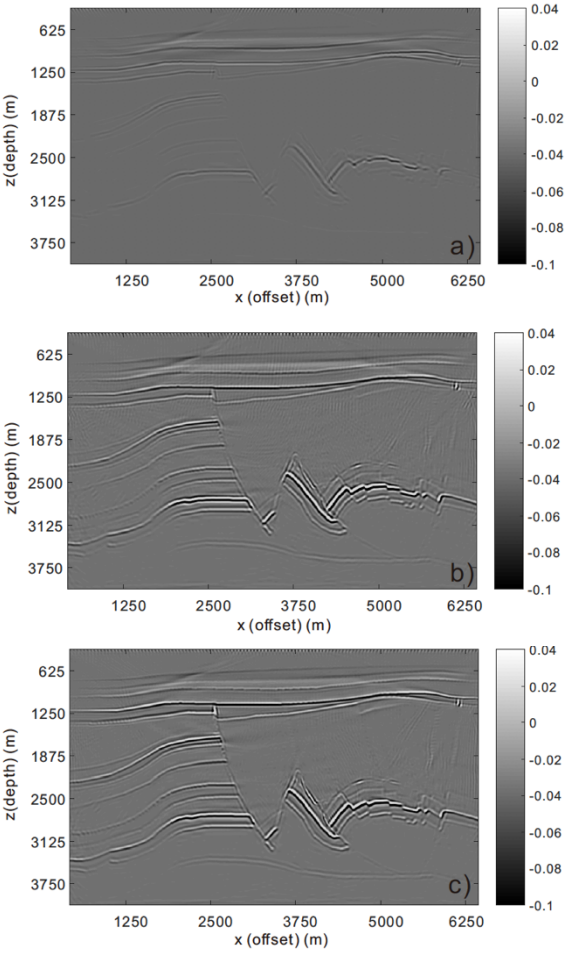

Figure 5. Q-RTM Imaging test of the BP 2007 TTI model with Q=40 in the shallow region (approximately between 625 - 1875 m). a) Conventional RTM with attenuated synthetic data; b) Broadband Q-RTM algorithm imaging result with attenuated synthetic data; c) Reference figure (RTM with un-attenuated synthetic data)

Conclusions and Discussions

We successfully developed a broadband finite-difference Q-compensated wave propagation engine for accurate Q-RTM applications by introducing integral optimization terms to correct the phase velocity in the low frequency band. This method can be applied to both general acoustic TI medium to enhance the imaging quality in complicated geological settings where visco-acoustic overburden is in presence. This algorithm utilizes only local numerical operators, saving the computational expense significantly. For the first time, the amplitude and the phase are compensated simultaneously with high accuracy in a wide frequency range (5 - 70 Hz), within the finite-difference Q-RTM engine. The numerical waveform recovery experiment validated the accuracy of this novel broadband Q-RTM algorithm. We conducted a numerical imaging test with the attenuated synthetics waveforms using part of the BP2007 TTI model with Q=40 in the shallow region. The broadband Q-RTM algorithm gives nearly identical image compared to the reference (Figure 5). The blurred and missing subsurface structure due to Q is successfully and accurately reconstructed.

References

Bickel, S.H. and Natarajan, R.R., 1985. Plane-wave Q deconvolution. Geophysics, 50(9), pp.1426-1439.

Blanch, J.O., Robertsson, J.O. and Symes, W.W., 1995. Modeling of a constant Q: Methodology and algorithm for an efficient and optimally inexpensive viscoelastic technique. Geophysics, 60(1), pp.176-184.

Dai, N. and West, G.F., 1994, January. Inverse Q migration. In 1994 SEG Annual Meeting. Society of Exploration Geophysicists.

Fletcher, R.P., Du, X. and Fowler, P.J., 2009. Reverse time migration in tilted transversely isotropic (TTI) media. Geophysics, 74(6), pp.WCA179-WCA187.

Guo, P., McMechan, G.A. and Guan, H., 2016. Comparison of two viscoacoustic propagators for Q-compensated reverse time migration. Geophysics, 81(5), pp.S281-S297.

Hargreaves, N.D. and Calvert, A.J., 1991. Inverse Q filtering by Fourier transform. Geophysics, 56(4), pp.519-527.

Hu, W., Zhou, T. and Ning, J., 2016. An efficient Q-RTM algorithm based on local differentiation operators. In SEG Technical Program Expanded Abstracts 2016 (pp. 4183-4187). Society of Exploration Geophysicists.

Hu W, Zhou T, and Ning J., 2017. Efficient Q-RTM in transversely isotropic media, In SEG Technical Program Expanded Abstracts 2017 (pp. 4676-4680). Society of Exploration Geophysicists.

Suh, S., Yoon, K., Cai, J. and Wang, B., 2012, November. Compensating visco-acoustic effects in anisotropic reverse-time migration. In 2012 SEG Annual Meeting. Society of Exploration Geophysicists.

Traynin, P., Liu, J. and Reilly, J.M., 2008, January. Amplitude and bandwidth recovery beneath gas zones using Kirchhoff prestack depth Q-migration. In 2008 SEG Annual Meeting. Society of Exploration Geophysicists.

Yu, Y., Lu, R.S. and Deal, M.M., 2002, January. Compensation for the effects of shallow gas attenuation with viscoacoustic wave-

equation migration. In SEG Technical Program Expanded Abstracts (Vol. 21, pp. 2062-2065).

Zhang, Y., Zhang, P. and Zhang, H., 2010, January. Compensating for visco-acoustic effects in reverse-time migration. In 2010 SEG Annual Meeting. Society of Exploration Geophysicists.

Zhou T., Hu W., and Ning J., 2018a, An efficient local operator-based Q-compensated reverse time migration algorithm with multistage optimization, Geophysics, 83(3), pp. S249-S259.

Zhou T., Hu W., and Ning J., 2018b, An attenuation compensation method in reverse time migration for visco-acoustic media. Chinese J. Geophys. (in Chinese), 61(6): 2433-2445

Zhu, T., Harris, J.M. and Biondi, B., 2014. Q-compensated reverse-time migration. Geophysics, 79(3), pp.S77-S87.